Vapor Pressure Measurements of NaHCOO + H_2O and KHCOO + H_2O from 278 to 308 K and Representation with an Ion Interaction (Pitzer) Model

Roland Beyer and Michael Steiger*

Department of Chemistry, University of Hamburg, Martin-Luther-King-Platz 6, 20146 Hamburg, Germany

The vapor pressures of NaHCOO(aq) and KHCOO(aq) were measured with a static method. For NaHCOO(aq), measurements were made from (278.15 to 308.15) K and from (0.54 to 12.9) mol·kg^{-1}. For KHCOO(aq), the measurements cover a temperature range from (278.15 to 323.15) K and extend from (1.03 to 38.8) mol·kg^{-1}. Published thermodynamic data for the two systems were reviewed, critically assessed, and used together with the present results to evaluate the parameters of a Pitzer-type ion interaction model. Published solubilities of NaHCOO·3H_2O, NaHCOO·2H_2O, NaHCOO, and KHCOO were used to evaluate the thermodynamic solubility products. The ion interaction model together with the solubility products allow for the calculation of solubilities and freezing temperatures in the systems (NaHCOO + H_2O) and (KHCOO + H_2O) from about (250 to 340) K.

Introduction

Because of their interesting physical and chemical properties, the alkali metal formates offer the potential for a number of useful applications. Many applications are based on the fact that aqueous sodium and potassium formate solutions are subject to catalytic decomposition under mild conditions into molecular hydrogen and bicarbonate.[1] This redox formate−bicarbonate cycle offers a number of potential industrial applications.[2,3] The cycle was also proposed as an efficient system for the generation and storage of hydrogen, that is, as an energy storage system.[4,5] These and other industrial processes[6] require detailed thermodynamic data of the formates. However, there is a lack of accurate data, and the present state of knowledge is quite inadequate.

Other applications of the formates include the use of potassium formate as a secondary refrigerant[7] and in absorption refrigeration,[8] and the use of both sodium formate and potassium formate as roadway and runway deicing salts. Compared to conventional deicers such as sodium chloride, these salts are less corrosive and have lower environmental toxicity.[9,10] Formic acid is among the most abundant organic acids in the atmosphere, and formates are major compounds of the water-soluble organic fraction of atmospheric aerosols.[11] Deposition of formic acid to buildings and the use of cleaning agents and deicing salts containing formic acid cause an enrichment of formate salts in building materials where they are ubiquitous constituents.[12] Once enriched in these porous materials, repeated crystallization and dissolution are a major cause of damage of such materials.[13] Formic acid is also a major pollutant in museum environments where its major source is emissions from wood used for the construction of display and storage cases.[14] In effect, the formation of formates on exposed artifacts is a major cause of damage.[15]

The measurements reported here form part of an ongoing investigation of the thermodynamic properties of aqueous acetate and formate solutions and their mixtures with common inorganic salts.[16,17] The major objective of these studies is the prediction of solubility equilibria in building materials and museum artifacts contaminated with complex mixtures of formates and acetates with inorganic salts.[18,19] This paper reports new vapor pressure measurements of (NaHCOO + H_2O) from (278.15 to 308.15) K and (0.54 to 12.91) mol·kg^{-1} and for (KHCOO + H_2O) from (278.15 to 323.15) K and (1.03 to 38.76 mol·kg^{-1}) mol·kg^{-1}. After critical evaluation, data from this work and available data from the literature are combined and treated with the equations of the Pitzer formalism to give a consistent representation of the thermodynamic properties of (NaHCOO + H_2O) and (KHCOO + H_2O) to about 330 K and from dilute solution to saturation.

Experimental Section

The vapor pressure apparatus was the same that was used in our previous work.[16] It consists of a glass sample flask in a thermostatted water bath connected to a vacuum pump and a capacitance manometer Baratron 220 (MKS Instruments) with a maximum operating pressure of 10 kPa and independently thermostatted at 318 K. The glass apparatus connecting the sample flask to the pressure gauge was covered with a heating wire, insulated, and maintained at 313 K to avoid condensation. The solution in the sample flask was stirred during the measurement with a magnetic stirrer. A Pt100 resistance thermometer in the water bath connected to the thermostat (model MH-4, Julabo) was used to control the bath temperature to within ± 0.01 K.

Analytical grade NaHCOO (Merck) and KHCOO (Fluka) were dried at 393 K for several days to constant weight. Subsequent analysis by acidimetric titration with sulfuric acid (0.5 mol·L^{-1}) confirmed that the samples were not completely dry but still contained residual water of 1.80 % (NaHCOO) and 4.02 % (KHCOO). Considering this residual water content, solutions were prepared by weighing appropriate amounts of the salts and water into a 100 mL flask to obtain the desired concentration. To degas the salt solutions, they were cooled, frozen in liquid nitrogen, and evacuated for several minutes. They were then allowed to warm under continuous evacuation.

* Corresponding author. Phone: +49 40 42838 2895. Fax: +49 40 42838 2893. E-mail: michael.steiger@chemie.uni-hamburg.de.

10.1021/je900487a CCC: $40.75
Published on Web 08/20/2009

This freeze−thaw cycling was repeated twice, and finally the solutions were evacuated for (30 to 60) min. Thereupon, the flask was lowered into the thermostatted water bath, and after the equilibrium temperature was attained, the vacuum valve was closed. Starting at 278.15 K, the temperature was increased stepwise in 5 K increments to 308.15 K or to 323.15 K in the case of the more concentrated KHCOO solutions. The upper temperature is limited by the maximum operating pressure of the capacitance manometer. Temperature was changed after equilibrium was reached, and the vapor pressure remained constant, which was normally the case after (30 to 45) min. After the end of the vapor pressure measurements the loss of water was determined by weighing the flask.

In our previous work it turned out that the pressure sensor should be calibrated to obtain maximum accuracy in water vapor pressure measurements. The calibration used in the present study was the same as in the previous work with ($NaCH_3COO + H_2O$).[16] After calibration, a maximum overall uncertainty of 0.24 % in the pressure measurements is estimated. Additional errors affecting the calculation of water activities a_w and osmotic coefficients ϕ include the uncertainties in the temperature and the molalities of the solutions. All temperature measurements were calibrated against a mercury thermometer with an uncertainty of 0.01 K yielding a maximum uncertainty of 0.14 % in the saturation water vapor pressure p_w° that is used for the calculation of the water activities of the solutions. The accuracy of the solution molalities is largely limited by the uncertainty in the residual water content after the drying procedure. A maximum error of 0.5 % is estimated for all solution molalities based on the uncertainty in the acidimetric titrations. A propagation of error analysis yields errors in the osmotic coefficients of 0.006 to 0.07 for NaHCOO(aq) and 0.005 to 0.04 for KHCOO(aq). The maximum errors result for low molalities where the error is largely controlled by the uncertainty of the pressure measurement. The best precision in the vapor pressure measurements is achieved at the highest molalities where the uncertainty of the solution molalities is the limiting factor.

Ion Interaction Equations

The osmotic coefficient ϕ of a solution of a 1−1 electrolyte is defined as:

$$\phi = -m_w \ln a_w/(2m) \quad (1)$$

where m_w is the molality of water (55.50844 mol·kg^{-1}) and m is the molality of the solute. In the Pitzer approach[20] the equation for the representation of the osmotic coefficient for a solution of a 1−1 type electrolyte MX is:

$$(\phi - 1) = f^\phi + (m/m^\circ)B^\phi_{MX} + (m/m^\circ)^2 C^\phi_{MX} \quad (2)$$

where m° denotes the unit molality of 1 mol·kg^{-1} and f^ϕ, the Debye−Hückel long-range electrostatic term, is given by:

$$f^\phi = -A_\phi I^{1/2}/(1 + bI^{1/2}) \quad (3)$$

where A_ϕ is the Debye−Hückel parameter for the osmotic coefficient, b is a constant ($b = 1.2$ kg$^{1/2}$·mol$^{-1/2}$), and I is the ionic strength, which for a 1−1 electrolyte is equivalent to the molality. B^ϕ_{MX} and C^ϕ_{MX} are the second and third virial coefficients in the ion interaction approach. B^ϕ_{MX} depends on the ionic strength

$$B^\phi_{MX} = \beta^{(0)}_{MX} + \beta^{(1)}_{MX}\exp(-\alpha_1 I^{1/2}) + \beta^{(2)}_{MX}\exp(-\alpha_2 I^{1/2}) \quad (4)$$

where the interaction parameters $\beta^{(0)}_{MX}$, $\beta^{(1)}_{MX}$, $\beta^{(2)}_{MX}$, and C^ϕ_{MX} are specific to the electrolyte MX, and α_1 and α_2 are numerical constants.

The mean activity coefficient γ_{MX} of a single 1−1 electrolyte solution in the ion interaction approach is given by

$$\ln \gamma_{MX} = f^\gamma + (m/m^\circ)B^\gamma_{MX} + (m/m^\circ)^2 C^\gamma_{MX} \quad (5)$$

where $C^\gamma_{MX} = 3/2 C^\phi_{MX}$ and the Debye−Hückel term f^γ for the activity coefficient is

$$f^\gamma = -A_\phi[I^{1/2}/(1 + bI^{1/2}) + 2/b \ln(1 + bI^{1/2})] \quad (6)$$

The function B^γ_{MX} is defined as

$$B^\gamma_{MX} = B_{MX} + B^\phi_{MX} \quad (7)$$

with

$$B_{MX} = \beta^{(0)}_{MX} + (2\beta^{(1)}_{MX}/\alpha_1^2 I)[1 - (1 + \alpha_1 I^{1/2})\exp(-\alpha_1 I^{1/2})] + (2\beta^{(2)}_{MX}/\alpha_2^2 I)[1 - (1 + \alpha_2 I^{1/2})\exp(-\alpha_2 I^{1/2})] \quad (8)$$

The ion interaction parameters $\beta^{(0)}_{MX}$, $\beta^{(1)}_{MX}$, $\beta^{(2)}_{MX}$, and C^ϕ_{MX} have to be determined from experimental data. Originally, the $\beta^{(2)}_{MX}$ term in eqs 4 and 8 was introduced for the treatment of the bivalent metal sulfates to avoid the explicit calculation of association equilibria.[21] As in our previous work,[22−24] we have included the $\beta^{(2)}_{MX}$ term in this study to enhance the numerical flexibility at very high concentrations.

To obtain the temperature dependence of the binary interaction parameters, experimental osmotic and activity coefficients at various temperatures and additional thermochemical data such as the apparent relative molar enthalpy ${}^\phi L$ and the apparent molar heat capacity ${}^\phi C_p$ may be used. The equation for the representation of the apparent relative molar enthalpy ${}^\phi L$ of a solution of a 1−1 electrolyte is

$${}^\phi L = (A_L/b)\ln(1 + bI^{1/2}) - 2RT^2[(m/m^\circ)B^L_{MX} + (m/m^\circ)^2 C^L_{MX}] \quad (9)$$

where R is the gas constant, T the absolute temperature, and A_L the Debye−Hückel parameter for enthalpy. Also, $C^L_{MX} = (\partial C_{MX}/\partial T)_p$ with $C_{MX} = C^\phi_{MX}/2$ in the case of a 1−1 type electrolyte. The function B^L_{MX} is given as:

$$B^L_{MX} = (\partial\beta^{(0)}_{MX}/\partial T)_p + (\partial\beta^{(1)}_{MX}/\partial T)_p g(\alpha_1 I^{1/2}) + (\partial\beta^{(2)}_{MX}/\partial T)_p g(\alpha_2 I^{1/2}) \quad (10)$$

with

$$g(\alpha_i I^{1/2}) = (2/\alpha_i^2 I)[1 - (1 + \alpha_i I^{1/2})\exp(-\alpha_i I^{1/2})] \quad (11)$$

Experimental data suitable for the determination of ${}^\phi L$ are heats of dilution and integral heats of solution. The integral heat of solution per mole of solute, ΔH_S, is related to ${}^\phi L$ through the enthalpy of solution per mole of salt at infinite dilution, ΔH_S°, by

$$\Delta H_S = \Delta H_S^\circ + {}^\phi L \quad (12)$$

where ΔH_S° is treated as an adjustable parameter. The enthalpy change on diluting a solution from molality m_1 to molality m_2 is given by

$$\Delta H_D = {}^\phi L_2 - {}^\phi L_1 \quad (13)$$

The equation for the apparent relative molar heat capacity ${}^\phi C_p$ of a solution of a 1−1 electrolyte is:

$$^{\phi}C_p = {}^{\phi}C_p^{\circ} + (A_J/b)\ln(1 + bI^{1/2}) - 2RT^2[(m/m^{\circ})B_{MX}^J + (m/m^{\circ})^2 C_{MX}^J] \quad (14)$$

where $^{\phi}C_p^{\circ}$ is the partial molar heat capacity of the solute at infinite dilution and A_J is the Debye−Hückel parameter for heat capacity. The functions B_{MX}^J and C_{MX}^J are defined as:

$$B_{MX}^J = (\partial B_{MX}^L/\partial T)_p + (2/T)B_{MX}^J \quad (15)$$

$$C_{MX}^J = (\partial C_{MX}^L/\partial T)_p + (2/T)C_{MX}^L \quad (16)$$

Hence, fitting apparent molar enthalpies and heat capacities yields the first and second temperature derivatives of the ion interaction parameters. The partial molar heat capacity at infinite dilution $^{\phi}C_p^{\circ}$ is treated as an adjustable parameter. It is also related to ΔH_S°:

$$^{\phi}C_p^{\circ} - C_p^{\circ}(s) = (\partial \Delta H_S^{\circ}/\partial T)_p \quad (17)$$

where $C_p^{\circ}(s)$ is the molar heat capacity of the anhydrous crystalline solids.

Results and Discussion

Vapor Pressure Measurements. The results of the vapor pressure measurements are listed in Tables 1 and 2 for (NaHCOO + H_2O) and (KHCOO + H_2O), respectively. Water activities were calculated from the vapor pressures p_w using the following equation:[25]

$$\ln a_w = \ln(p_w/p_w^{\circ}) + B_2(T)(p_w - p_w^{\circ})/RT + V_{w,l}^{\circ}(p_w^{\circ} - p_w)/RT \quad (18)$$

where $B_2(T)$ is the second virial coefficient of water vapor and $V_{w,l}^{\circ}$ is the molar volume of liquid water. An equation for the second virial coefficient is provided by Rard and Platford.[25] Molar volumes and saturation pressures of liquid water were calculated using the equations of Kell[26] and Saul and Wagner,[27] respectively. Osmotic coefficients were calculated using eq 1. As in the case of $NaCH_3COO$(aq),[16] the water activity shows a small but approximately linear temperature dependence. Because of the very high solubility of KHCOO the measurements extend to very low water activities of about 0.21 at $m = 38.8$ mol·kg^{-1} and 303 K.

Figure 1 depicts the osmotic coefficients in NaHCOO solutions at 298.15 K calculated from our vapor pressure data together with available isopiestic data.[28,29] Generally, our data agree with the isopiestic data to within the combined experimental uncertainties. Only at low molalities where the accuracy of the pressure sensor is the limiting factor, it appears that the vapor pressure data are systematically low. At molalities above about 1 mol·kg^{-1}, the experimental uncertainty is significantly lower, and there is good agreement with the isopiestic data. No isopiestic or other data are available for KHCOO(aq) in the temperature range of the present study.

Thermodynamic Data for NaHCOO(aq) and KHCOO(aq). The data used for the determination of the ion interaction parameters for NaHCOO(aq) are listed in Table 3. Smith and Robinson[28] reported isopiestic data from (0.6486 to 3.373) mol·kg^{-1} at 298.15 K with KCl(aq) as the reference standard. Osmotic coefficients were calculated from the isopiestic molalities using the equation of Archer.[30] Bonner[29] reported isopiestic molalities of NaHCOO(aq) [(2.9 to 14.7) mol·kg^{-1}] and LiCl(aq) which is not one of the traditional reference standards for isopiestic measurements. The osmotic coefficients of NaHCOO(aq) were calculated using the equation of Hamer and Wu[31] for LiCl(aq). It is expected that this equation has significantly larger uncertainties than more recent equations for the traditional reference standards. Nonetheless, the osmotic coefficients of NaHCOO(aq) at 298.15 K from the two isopiestic studies[28,29] and the present vapor pressure measurements show reasonable agreement and appear to be a consistent database (Figure 1).

The vapor pressure measurements of the present work are the most important source of data for the determination of the temperature dependence of the ion interaction parameters of (NaHCOO + H_2O) at near ambient temperatures. For the reason

Table 1. Water Vapor Pressures *p*, Water Activities a_w, and Osmotic Coefficients ϕ of NaHCOO + H_2O at Molality *m* and Temperature *T*

T/K	*p*/kPa	a_w	ϕ	*T*/K	*p*/kPa	a_w	ϕ
$m = 0.5351$ mol·kg^{-1}[a]				$m = 1.0901$ mol·kg^{-1}			
278.15	0.858	0.9840	0.837	278.15	0.841	0.9641	0.932
283.15	1.209	0.9846	0.805	283.15	1.185	0.9647	0.915
288.15	1.678	0.9841	0.830	288.15	1.645	0.9646	0.917
293.15	2.302	0.9844	0.817	293.15	2.255	0.9644	0.924
298.15	3.118	0.9841	0.830	298.15	3.056	0.9645	0.920
303.15	4.177	0.9840	0.838	303.15	4.094	0.9645	0.921
308.15	5.534	0.9836	0.859	308.15	5.424	0.9641	0.931
$m = 1.9928$ mol·kg^{-1}				$m = 2.7865$ mol·kg^{-1}			
278.15	0.815	0.9338	0.955	278.15	0.792	0.9074	0.968
283.15	1.148	0.9347	0.940	283.15	1.114	0.9070	0.972
288.15	1.592	0.9338	0.954	288.15	1.545	0.9064	0.979
293.15	2.183	0.9335	0.958	293.15	2.118	0.9059	0.984
298.15	2.957	0.9332	0.962	298.15	2.868	0.9054	0.990
303.15	3.960	0.9331	0.965	303.15	3.841	0.9050	0.994
308.15	5.248	0.9329	0.967	308.15	5.088	0.9045	1.000
$m = 3.4499$ mol·kg^{-1}				$m = 3.6396$ mol·kg^{-1}			
278.15	0.769	0.8812	1.018	278.15	0.763	0.8745	1.022
283.15	1.082	0.8809	1.020	283.15	1.074	0.8747	1.021
288.15	1.502	0.8812	1.018	288.15	1.491	0.8745	1.023
293.15	2.059	0.8807	1.022	293.15	2.044	0.8744	1.024
298.15	2.790	0.8806	1.023	298.15	2.769	0.8742	1.026
303.15	3.736	0.8803	1.026	303.15	3.709	0.8739	1.028
308.15	4.951	0.8802	1.027	308.15	4.914	0.8737	1.030
$m = 4.4844$ mol·kg^{-1}				$m = 5.6153$ mol·kg^{-1}			
278.15	0.736	0.8432	1.055	278.15	0.700	0.8025	1.088
283.15	1.035	0.8430	1.057	283.15	0.986	0.8028	1.085
288.15	1.437	0.8428	1.058	288.15	1.368	0.8025	1.087
293.15	1.971	0.8429	1.058	293.15	1.877	0.8029	1.085
298.15	2.670	0.8428	1.058	298.15	2.544	0.8031	1.084
303.15	3.576	0.8426	1.060	303.15	3.407	0.8030	1.085
308.15	4.740	0.8428	1.058	308.15	4.517	0.8032	1.083
$m = 6.6365$ mol·kg^{-1}				$m = 7.0478$ mol·kg^{-1}[a]			
278.15	0.667	0.7647	1.122	278.15	0.658	0.7539	1.113
283.15	0.939	0.7646	1.122	283.15	0.926	0.7542	1.111
288.15	1.305	0.7653	1.118	288.15	1.284	0.7534	1.115
293.15	1.790	0.7657	1.116	293.15	1.763	0.7543	1.111
298.15	2.427	0.7662	1.114	298.15	2.393	0.7554	1.105
303.15	3.255	0.7672	1.108	303.15	3.207	0.7557	1.103
308.15	4.318	0.7678	1.105	308.15	4.255	0.7567	1.098
$m = 8.0738$ mol·kg^{-1}				$m = 9.7921$ mol·kg^{-1}			
283.15	0.879	0.7161	1.148	288.15	1.136	0.6663	1.151
288.15	1.222	0.7171	1.143	293.15	1.561	0.6679	1.144
293.15	1.680	0.7185	1.136	298.15	2.121	0.6696	1.137
298.15	2.280	0.7198	1.130	303.15	2.849	0.6715	1.129
303.15	3.059	0.7210	1.124	308.15	3.786	0.6734	1.121
308.15	4.062	0.7225	1.117				
$m = 9.8008$ mol·kg^{-1}				$m = 10.8369$ mol·kg^{-1}			
288.15	1.128	0.6617	1.170	293.15	1.489	0.6370	1.155
293.15	1.552	0.6641	1.159	298.15	2.024	0.6392	1.146
298.15	2.110	0.6661	1.150	303.15	2.721	0.6414	1.137
303.15	2.835	0.6683	1.141	308.15	3.619	0.6437	1.128
308.15	3.771	0.6707	1.131				
$m = 11.7914$ mol·kg^{-1}				$m = 12.9102$ mol·kg^{-1}			
293.15	1.431	0.6124	1.154	298.15	1.867	0.5895	1.136
298.15	1.945	0.6143	1.147	303.15	2.515	0.5929	1.124
303.15	2.619	0.6174	1.135	308.15	3.350	0.5959	1.113
308.15	3.487	0.6202	1.124	313.15	4.408	0.5978	1.106

[a] Not included in fit.

Table 2. Water Vapor Pressures p, Water Activities a_w, and Osmotic Coefficients ϕ of KHCOO + H_2O at Molality m and Temperature T

T/K	p/kPa	a_w	ϕ	T/K	p/kPa	a_w	ϕ	T/K	p/kPa	a_w	ϕ	T/K	p/kPa	a_w	ϕ
m = 1.0298 mol·kg^{-1}				m = 1.0298 mol·kg^{-1}				m = 1.8532 mol·kg^{-1}				m = 1.8532 mol·kg^{-1}			
278.15	0.843	0.9665	0.9180	298.15	3.060	0.9659	0.9350	278.15	0.817	0.9362	0.9880	298.15	2.964	0.9354	1.0000
283.15	1.187	0.9664	0.9210	303.15	4.099	0.9656	0.9430	283.15	1.150	0.9364	0.9830	303.15	3.970	0.9352	1.0030
288.15	1.648	0.9665	0.9170	308.15	5.430	0.9652	0.9550	288.15	1.596	0.9360	0.9910	308.15	5.260	0.9350	1.0070
293.15	2.259	0.9660	0.9330					293.15	2.188	0.9355	0.9980				
m = 2.6635 mol·kg^{-1}				m = 2.6635 mol·kg^{-1}				m = 3.3345 mol·kg^{-1}				m = 3.3345 mol·kg^{-1}			
278.15	0.789	0.9042	1.0490	298.15	2.865	0.9044	1.0470	278.15	0.766	0.8776	1.0870	298.15	2.777	0.8766	1.0960
283.15	1.111	0.9050	1.0410	303.15	3.839	0.9044	1.0470	283.15	1.077	0.8773	1.0900	303.15	3.720	0.8765	1.0970
288.15	1.543	0.9049	1.0410	308.15	5.086	0.9041	1.0500	288.15	1.495	0.8769	1.0940	308.15	4.929	0.8764	1.0980
293.15	2.115	0.9047	1.0440					293.15	2.050	0.8766	1.0960				
m = 4.5918 mol·kg^{-1}				m = 4.5918 mol·kg^{-1}				m = 4.8215 mol·kg^{-1}				m = 4.8215 mol·kg^{-1}			
278.15	0.719	0.8241	1.1690	298.15	2.609	0.8237	1.1720	278.15	0.709	0.8123	1.1960	298.15	2.582	0.8151	1.1770
283.15	1.011	0.8237	1.1720	303.15	3.495	0.8236	1.1730	283.15	1.000	0.8141	1.1840	303.15	3.459	0.8151	1.1770
288.15	1.404	0.8235	1.1740	308.15	4.634	0.8239	1.1710	288.15	1.389	0.8147	1.1790	308.15	4.585	0.8153	1.1760
293.15	1.926	0.8236	1.1730					293.15	1.905	0.8149	1.1780				
m = 5.5182 mol·kg^{-1}				m = 5.5182 mol·kg^{-1}				m = 6.8204 mol·kg^{-1}				m = 6.8204 mol·kg^{-1}			
278.15	0.684	0.7845	1.2210	298.15	2.487	0.7853	1.2160	278.15	0.635	0.7284	1.2900	298.15	2.318	0.7317	1.2710
283.15	0.963	0.7847	1.2190	303.15	3.333	0.7854	1.2150	283.15	0.896	0.7298	1.2820	303.15	3.108	0.7324	1.2670
288.15	1.338	0.7847	1.2200	308.15	4.418	0.7856	1.2140	288.15	1.245	0.7305	1.2780	308.15	4.122	0.7330	1.2640
293.15	1.835	0.7848	1.2190					293.15	1.709	0.7311	1.2740				
m = 7.6488 mol·kg^{-1}				m = 7.6488 mol·kg^{-1}				m = 8.3137 mol·kg^{-1}				m = 8.3137 mol·kg^{-1}			
278.15	0.606	0.6948	1.3210	298.15	2.213	0.6988	1.3010	278.15	0.583	0.6683	1.3450	298.15	2.135	0.6742	1.3160
283.15	0.855	0.6963	1.3140	303.15	2.969	0.6998	1.2950	283.15	0.824	0.6715	1.3300	303.15	2.865	0.6754	1.3100
288.15	1.188	0.6971	1.3090	308.15	3.940	0.7007	1.2910	288.15	1.145	0.6719	1.3270	308.15	3.802	0.6763	1.3060
293.15	1.632	0.6980	1.3050					293.15	1.573	0.6730	1.3220				
m = 8.935 mol·kg^{-1}				m = 8.935 mol·kg^{-1}				m = 10.175 mol·kg^{-1}				m = 10.175 mol·kg^{-1}			
278.15	0.563	0.6457	1.3590	298.15	2.065	0.6519	1.3290	278.15	0.525	0.6015	1.3870	298.15	1.927	0.6085	1.3550
283.15	0.796	0.6482	1.3470	303.15	2.770	0.6530	1.3240	283.15	0.741	0.6040	1.3750	303.15	2.587	0.6099	1.3490
288.15	1.107	0.6491	1.3420	308.15	3.676	0.6539	1.3190	288.15	1.032	0.6056	1.3680	308.15	3.435	0.6111	1.3430
293.15	1.521	0.6507	1.3350					293.15	1.419	0.6070	1.3620	313.15	4.507	0.6112	1.3430
m = 11.765 mol·kg^{-1}				m = 11.765 mol·kg^{-1}				m = 13.372 mol·kg^{-1}				m = 13.372 mol·kg^{-1}			
278.15	0.480	0.5502	1.4090	298.15	1.769	0.5587	1.3730	278.15	0.440	0.5041	1.4220	298.15	1.627	0.5137	1.3830
283.15	0.679	0.5530	1.3980	303.15	2.377	0.5605	1.3660	283.15	0.623	0.5079	1.4060	303.15	2.187	0.5157	1.3740
288.15	0.946	0.5549	1.3890	308.15	3.161	0.5624	1.3580	288.15	0.868	0.5094	1.4000	308.15	2.910	0.5178	1.3660
293.15	1.302	0.5569	1.3810					293.15	1.196	0.5116	1.3910	313.15	3.825	0.5189	1.3610
m = 14.325 mol·kg^{-1}				m = 14.325 mol·kg^{-1}				m = 15.910 mol·kg^{-1}				m = 15.910 mol·kg^{-1}			
278.15	0.418	0.4793	1.4250	303.15	2.088	0.4923	1.3730	278.15	0.386	0.4430	1.4200	303.15	1.926	0.4541	1.3770
283.15	0.592	0.4825	1.4120	308.15	2.779	0.4945	1.3640	283.15	0.547	0.4456	1.4100	308.15	2.564	0.4563	1.3690
288.15	0.828	0.4857	1.3990	313.15	3.652	0.4955	1.3600	288.15	0.763	0.4479	1.4010	313.15	3.374	0.4577	1.3630
293.15	1.140	0.4878	1.3910	318.15	4.755	0.4966	1.3560	293.15	1.051	0.4498	1.3940	318.15	4.395	0.4591	1.3580
298.15	1.552	0.4902	1.3810					298.15	1.431	0.4520	1.3850				
m = 17.875 mol·kg^{-1}				m = 17.875 mol·kg^{-1}				m = 18.362 mol·kg^{-1}				m = 18.362 mol·kg^{-1}			
278.15	0.350	0.4010	1.4190	303.15	1.761	0.4152	1.3650	278.15	0.344	0.3942	1.4070	303.15	1.728	0.4076	1.3570
283.15	0.497	0.4046	1.4050	308.15	2.347	0.4176	1.3560	283.15	0.487	0.3971	1.3960	308.15	2.305	0.4101	1.3470
288.15	0.695	0.4078	1.3930	313.15	3.089	0.4192	1.3500	288.15	0.682	0.4002	1.3840	313.15	3.034	0.4117	1.3410
293.15	0.959	0.4103	1.3830	318.15	4.027	0.4208	1.3440	293.15	0.941	0.4025	1.3760	318.15	3.957	0.4134	1.3350
298.15	1.307	0.4129	1.3730					298.15	1.283	0.4053	1.3650				
m = 20.469 mol·kg^{-1}				m = 20.469 mol·kg^{-1}				m = 22.005 mol·kg^{-1}				m = 22.005 mol·kg^{-1}			
278.15	0.311	0.3569	1.3970	303.15	1.577	0.3719	1.3410	278.15	0.293	0.3355	1.3780	303.15	1.482	0.3496	1.3260
283.15	0.443	0.3610	1.3810	308.15	2.102	0.3741	1.3330	283.15	0.416	0.3386	1.3660	308.15	1.978	0.3521	1.3170
288.15	0.621	0.3643	1.3690	313.15	2.769	0.3758	1.3270	288.15	0.582	0.3416	1.3550	313.15	2.608	0.3539	1.3100
293.15	0.857	0.3668	1.3600	318.15	3.612	0.3774	1.3210	293.15	0.805	0.3445	1.3440	318.15	3.403	0.3556	1.3040
298.15	1.169	0.3693	1.3510	323.15	4.669	0.3791	1.3150	298.15	1.099	0.3470	1.3350				
m = 24.211 mol·kg^{-1}				m = 24.211 mol·kg^{-1}				m = 24.995 mol·kg^{-1}				m = 24.995 mol·kg^{-1}			
278.15	0.268	0.3070	1.3540	303.15	1.365	0.3219	1.3000	278.15	0.259	0.2968	1.3490	303.15	1.323	0.3121	1.2930
283.15	0.381	0.3107	1.3400	308.15	1.821	0.3241	1.2920	283.15	0.369	0.3008	1.3340	308.15	1.766	0.3143	1.2850
288.15	0.535	0.3137	1.3290	313.15	2.402	0.3260	1.2850	288.15	0.518	0.3041	1.3220	313.15	2.330	0.3162	1.2790
293.15	0.740	0.3166	1.3180	318.15	3.136	0.3278	1.2790	293.15	0.718	0.3071	1.3110	318.15	3.043	0.3180	1.2720
298.15	1.010	0.3192	1.3090	323.15	4.058	0.3296	1.2720	298.15	0.980	0.3094	1.3020	323.15	3.940	0.3200	1.2650
m = 26.771 mol·kg^{-1}				m = 26.771 mol·kg^{-1}				m = 29.334 mol·kg^{-1}				m = 29.334 mol·kg^{-1}			
278.15	0.240	0.2752	1.3380	303.15	1.233	0.2909	1.2800	278.15	0.222	0.2545	1.2950	303.15	1.141	0.2692	1.2420
283.15	0.343	0.2795	1.3210	308.15	1.648	0.2934	1.2710	283.15	0.317	0.2584	1.2800	308.15	1.527	0.2718	1.2320
288.15	0.482	0.2827	1.3100	313.15	2.175	0.2952	1.2650	288.15	0.445	0.2614	1.2690	313.15	2.016	0.2736	1.2260
293.15	0.668	0.2858	1.2980	318.15	2.842	0.2970	1.2590	293.15	0.617	0.2642	1.2590	318.15	2.635	0.2754	1.2200
298.15	0.913	0.2883	1.2890	323.15	3.680	0.2989	1.2520	298.15	0.844	0.2668	1.2500	323.15	3.414	0.2773	1.2130
m = 29.818 mol·kg^{-1}				m = 29.818 mol·kg^{-1}				m = 30.529 mol·kg^{-1}				m = 30.529 mol·kg^{-1}			
278.15	0.217	0.2486	1.2960	303.15	1.121	0.2643	1.2380	278.15	0.212	0.2432	1.2850	303.15	1.092	0.2576	1.2330
283.15	0.311	0.2532	1.2790	308.15	1.500	0.2670	1.2290	283.15	0.303	0.2466	1.2730	308.15	1.461	0.2600	1.2250
288.15	0.437	0.2563	1.2670	313.15	1.980	0.2687	1.2230	288.15	0.426	0.2499	1.2610	313.15	1.929	0.2619	1.2180
293.15	0.606	0.2592	1.2570	318.15	2.590	0.2707	1.2160	293.15	0.590	0.2527	1.2500	318.15	2.522	0.2636	1.2120
298.15	0.829	0.2619	1.2470	323.15	3.355	0.2726	1.2100	298.15	0.808	0.2553	1.2410	323.15	3.267	0.2654	1.2060
m = 33.458 mol·kg^{-1}				m = 33.458 mol·kg^{-1}				m = 33.797 mol·kg^{-1}				m = 33.797 mol·kg^{-1}			
278.15	0.193	0.2219	1.2490	303.15	1.005	0.2372	1.1940	288.15	0.381	0.2233	1.2310	308.15	1.311	0.2333	1.1950
283.15	0.277	0.2257	1.2350	308.15	1.345	0.2395	1.1850	293.15	0.528	0.2260	1.2210	313.15	1.732	0.2351	1.1890
288.15	0.391	0.2295	1.2210	313.15	1.777	0.2412	1.1800	298.15	0.724	0.2287	1.2120	318.15	2.267	0.2369	1.1830
293.15	0.542	0.2321	1.2110	318.15	2.325	0.2430	1.1740	303.15	0.980	0.2311	1.2030	323.15	2.939	0.2388	1.1760
298.15	0.743	0.2348	1.2020	323.15	3.014	0.2448	1.1670								

Table 2.. Continued

T/K	p/kPa	a_w	ϕ	T/K	p/kPa	a_w	ϕ	T/K	p/kPa	a_w	ϕ	T/K	p/kPa	a_w	ϕ
m = 34.148 mol·kg^{-1}				m = 34.148 mol·kg^{-1}				m = 38.764 mol·kg^{-1}				m = 38.764 mol·kg^{-1}			
288.15	0.381	0.2239	1.2160	308.15	1.315	0.2341	1.1800	303.15	0.878	0.2072	1.1270	318.15	2.030	0.2123	1.1100
293.15	0.530	0.2269	1.2050	313.15	1.736	0.2357	1.1750	308.15	1.172	0.2088	1.1220	323.15	2.634	0.2140	1.1040
298.15	0.726	0.2293	1.1970	318.15	2.272	0.2375	1.1680	313.15	1.551	0.2106	1.1150				
303.15	0.983	0.2318	1.1880	323.15	2.946	0.2393	1.1620								

given before, the measurements at the lowest molality (0.5351 mol·kg^{-1}) were not included in the data treatment. Also, the values of ϕ determined from the series of measurements at m = 7.048 mol·kg^{-1} appear to be systematically low and were not included in the fit. Tammann[32] reported additional vapor pressures at 373 K and (1.566 to 22.06) mol·kg^{-1}. Osmotic coefficients were calculated from these data using eq 18. Though the data are expected to be less accurate than the remaining data, they proved to be helpful to guide the fit at high concentration and enhanced temperatures.

Peng and Chan[11] reported results of vapor pressure measurements of levitated solution droplets with an electrodynamic balance (edb) at 298.15 K. Electrodynamic balance measurements extend far into the supersaturated molality region; for example, Peng and Chan reported results to 44.5 mol·kg^{-1} for NaHCOO(aq). Usually, in edb measurements the molality in the levitated droplets is not measured directly but is rather obtained by normalization. Peng and Chan normalized their edb

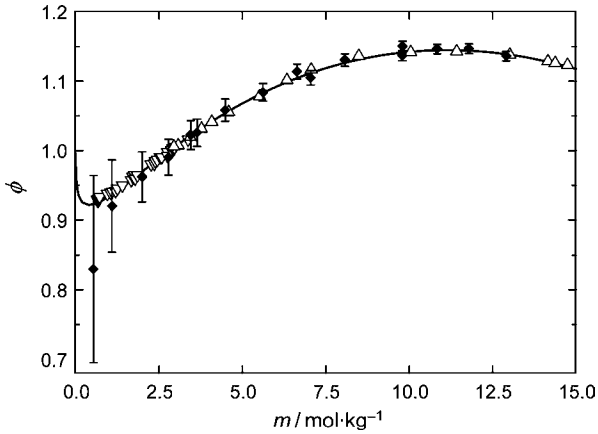

Figure 1. Experimental osmotic coefficients of NaHCOO(aq) at 298.15 K. Sources of data are: isopiestic data of Smith and Robinson[28] (▽) and Bonner[29] (△), vapor pressure measurements of the present research (♦); lines represent predicted values using the model.

Table 3. Thermodynamic Database for NaHCOO(aq)

property[a]	T/K	m/mol·kg^{-1}	N^b	$\sigma_{est}{}^c$	$\sigma_{fit}{}^d$	ref
ϕ(iso)	298	0.65−3.4	30 (30)	0.003	0.002	28
ϕ(iso)	298	2.9−14.7	16 (16)	0.01	0.003	29
ϕ(vp)	278−313	0.5−12.9	84 (98)	0.006−0.07	0.008	this work
ϕ(vp)	373	1.6−22.1	10 (11)	0.025	0.014	32
ϕ(edb)	298	0.1−44.5	0[e]	0.04−0.1		11
ϕ(ft)	255−269	1.1−4.9	0 (4)	0.02−0.09		33
ϕ(ft)	268−273	0.002−1.4	29 (29)	0.003−0.006	0.0015	34
$^{\phi}L$ (ΔH_D)	298	0.025−2.5	1 (1)	10	45	36
$^{\phi}L$ (ΔH_S)	298	0.12−0.15	5 (5)	12	7	36
$^{\phi}L$ (ΔH_S)	298, 308	0.001	1 (2)	146	59	37
$^{\phi}C_P$	273−393	0.5−2.9	39 (39)	8−43	12	38

[a] Fitted quantity and experimental technique (iso = isopiestic, vp = vapor pressure, edb = electrodynamic balance, and ft = freezing temperature). [b] Number of experimental data used in fit (total number of observations in brackets). [c] Assigned standard error. [d] Standard error of fit. [e] The exact number of data points is unknown since only a correlating equation was reported.

Table 4. Thermodynamic Database for KHCOO(aq)

property[a]	T/K	m/mol·kg^{-1}	N^b	$\sigma_{est}{}^c$	$\sigma_{fit}{}^d$	ref
ϕ(vp)	278−323	1.0−38.8	239 (246)	0.005−0.04	0.007	this work
ϕ(vp)	373	1.0−7.5	8 (12)	0.02−0.07	0.015	32
ϕ(ft)	256−271	0.7−4.2	0 (5)	0.02−0.09		33
ϕ(ft)	269−273	0.0009−1.2	28 (28)	0.003−0.01	0.02	34
ϕ(ft)	228−268	1.4−9.2	0 (9)	0.05−0.4		7

[a] Fitted quantity and experimental technique (vp = vapor pressure, ft = freezing temperature). [b] Number of experimental data used in fit (total number of observations in brackets). [c] Assigned standard error. [d] Standard error of fit.

data such that their water activities at low molalities are in agreement with the smoothed isopiestic data of Smith and Robinson[28] as tabulated by Hamer and Wu[31] and presented a correlating equation for $0.99 < a_w < 0.29$. Osmotic coefficients calculated from their data are systematically higher than the osmotic coefficients from both the isopiestic data of Bonner[29] and the vapor pressure measurements of the present work. Therefore, the edb data were not included in the fit.

Freezing temperature depressions for NaHCOO(aq) were reported by Sidgwick and Gentle[33] and Scatchard and Prentiss.[34] Osmotic coefficients were calculated from these data using the equation of Klotz and Rosenberg.[35] The osmotic coefficients calculated from the data of Sidgwick and Gentle[33] are not consistent with the remaining data and were not included in the fit.

Only few thermochemical measurements are available for NaHCOO(aq). Snell and Greyson[36] reported a single heat of dilution value from (2.5 to 0.025) mol·kg^{-1} at 298.15 K. The same authors have also reported heat of solution measurements at (0.12 to 0.15) mol·kg^{-1}. Chawla and Ahluwalia[37] reported two heat of solution measurements for very dilute solutions (0.001 mol·kg^{-1}) at 298.15 K. Ackermann and Schreiner[38] reported heat capacities for (0.5 to 2.9) mol·kg^{-1} NaHCOO(aq) from (273.15 to 393.15) K. These heat capacities were converted to apparent molar heat capacities $^{\phi}C_p$ using heat capacities of pure water taken from Kell.[39] Westrum et al.[40] and Franzosini et al.[41] reported heat capacities of NaHCOO(cr) that were helpful together with the heat of solutions as an additional source of data for the determination of the partial molar heat capacities at infinite dilution.

The thermodynamic data used in the determination of the model parameters for KHCOO(aq) are listed in Table 4. Freezing temperature depressions for KHCOO(aq) were reported by Sidgwick and Gentle,[33] Scatchard and Prentiss,[34] and Aittomäki and Lahti.[7] Osmotic coefficients were calculated from these data using the equation of Klotz and Rosenberg.[35] Apart from the very accurate data of Scatchard and Prentiss,[34] the remaining data are substantially scattered and were not included in the least-squares treatment. As in the case of NaHCOO(aq), osmotic coefficients were calculated from the vapor pressures of Tammann[32] using eq 18, and 8 out of the 12 values were included in the fit to constrain the model at high temperatures. All vapor pressure measurements of the present study were included in the final fit.

Apart from the vapor pressure measurements of the present study, there are only two additional sources of data that could be used in the least-squares treatment, the freezing temperatures of Scatchard and Prentiss[34] and the vapor pressures of Tammann.[32] These data cover a temperature range from (268 to 373) K. However, many applications of potassium formate, for example, as a secondary refrigerant or deicing salt, require thermodynamic data down to at least 220 K. While it was found that the model equation for NaHCOO(aq) provides reasonable extrapolation to low temperatures (see discussion below), test calculations have shown that this was not the case for KHCOO(aq). To constrain the model at low temperatures we made use of the fact that the water activities of KHCOO(aq) show a nearly linear dependence on temperature. Water activity isotherms were calculated at (198, 223 and 248) K by extrapolation of linear fits of the experimental water activities at (278.15 to 308.15) K. Osmotic coefficients were calculated, and the data were included in the least-squares treatment.

Determination of Model Parameters for NaHCOO(aq) and KHCOO(aq). Beyer and Steiger[16] were able to represent accurately the thermodynamic properties of $NaCH_3COO$(aq) to high molalities using the extended equation with the $\beta^{(2)}_{MX}$ term. The same approach is used in the present treatment. As in our earlier work, the following temperature-dependent expression $P(T)$ for each parameter $\beta^{(0)}_{MX}$, $\beta^{(1)}_{MX}$, $\beta^{(2)}_{MX}$, and C^{ϕ}_{MX} is also adopted in the present work:

$$P(T) = q_1 + q_2(1/T - 1/T_R)T^\circ + q_3 \ln(T/T_R) + q_4(T - T_R)/T^\circ + q_5(T^2 - T_R^2)/T^{\circ 2} + q_6 \ln[(T - T_C)/T^\circ)] \quad (19)$$

with $T_R = 298.15$ K, $T_C = 150$ K, and $T^\circ = 1$ K. The temperature dependence of the remaining parameters, that is, ΔH°_S, ${}^{\phi}C^\circ_p$, and C°_p(s), is represented by the following equations:

$$\Delta H^\circ_S = p_1 + p_2 T/T^\circ + p_3(T/T^\circ)^2 + p_4 \ln(T/T^\circ) \quad (20)$$

$$C^\circ_p(\mathrm{s}) = p_5 + p_6 T/T^\circ + p_7(T/T^\circ)^2 \quad (21)$$

Hence, according to eq 17

$${}^{\phi}C^\circ_p = C^\circ_p(\mathrm{s}) + p_2 + 2p_3 T/T^\circ + p_4(T^\circ/T)^2 \quad (22)$$

To properly weight the different types of experimental data in the least-squares treatment, the estimated standard errors listed in column 5 of Tables 3 and 4 were used. The error estimates are based on the reported experimental errors, the internal consistency and scatter of each data set, and the compatibility with the remaining data sets. The weighting of the low temperature data calculated by extrapolation was such that the reproduction of the experimental data at higher temperatures was not significantly affected.

In the case of NaHCOO(aq), the parameters p_5, p_6, and p_7 were determined first by a separate fit of the heat capacities of NaHCOO(cr)[40,41] to eq 21. These parameters were then used to fix C°_p(s) in eq 22 for the simultaneous least-squares fit of the remaining parameters in eqs 19, 20, and 22. Since no thermochemical data are available for KHCOO(aq), the temperature dependence of the ion interaction parameters were determined exclusively from the variation of the osmotic coefficients with temperature.

The values of α_1 and α_2 were fixed after trial calculations. Values of $\alpha_1 = 3.0$ kg$^{1/2}$·mol$^{-1/2}$ and $\alpha_2 = 0.5$ kg$^{1/2}$·mol$^{-1/2}$ were selected for NaHCOO(aq), while $\alpha_1 = 1.0$ kg$^{1/2}$·mol$^{-1/2}$ and $\alpha_2 = 0.5$ kg$^{1/2}$·mol$^{-1/2}$ proved more appropriate for KHCOO(aq). Values of the Debye−Hückel parameters, A_ϕ, A_L, and A_J, are those determined by Archer and Wang.[42] A simple equation representing the temperature dependence of A_ϕ at 0.1 MPa in the temperature range (238 to 473) K was provided recently.[23] This equation was used to a low temperature limit of 245 K in the present work. Below 245 K values of A_ϕ were obtained by linear extrapolation yielding

$$A_\phi = a_1 + a_2(T - 245\ \mathrm{K})/T^\circ \quad (23)$$

where $a_1 = 0.356370$ kg$^{1/2}$·mol$^{-1/2}$ and $a_2 = 0.00132115$ kg$^{1/2}$·mol$^{-1/2}$.

The final model parameters for NaHCOO(aq) and KHCOO(aq) are listed in Tables 5 and 6. Tables 3 and 4 list the standard errors of the fit for the individual data sets. Most of the data are reproduced to well within their respective experimental uncertainties. Figure 2 depicts the deviations of the experimental osmotic coefficients of NaHCOO(aq) from the ion interaction model. The deviations from the model are completely random, and the deviations do not exceed the experimental uncertainties. Figure 3 illustrates the deviations of the experimental osmotic coefficients for KHCOO(aq). While there is agreement to within the experimental uncertainties of the vapor pressure measurements, there is a weak cyclic variation of the residuals of the freezing temperature data, that is, at molalities < 1.2 mol·kg^{-1}. Hence, at low molalities the deviations of the model predictions slightly exceed the experimental uncertainty. Nonetheless, considering the extremely high molalities to 38.8 mol·kg^{-1} in the potassium formate solutions, the reproduction of the experimental data by the model appears to be quite satisfactory and will be useful in many practical applications.

Solubilities. The thermodynamic solubility product of a hydrated solid MX·ν_0H$_2$O of a 1−1 electrolyte is given by

Table 5. Parameters of eq 19 for NaHCOO(aq) and KHCOO(aq)

$P(T)$		NaHCOO(aq)	KHCOO(aq)
$\beta^{(0)}$	q_1	$3.69993 \cdot 10^{-2}$	$1.25149 \cdot 10^{0}$
	q_2	$3.89855 \cdot 10^{1}$	$-1.82903 \cdot 10^{3}$
	q_3		$-1.26523 \cdot 10^{1}$
	q_4		$2.35071 \cdot 10^{-2}$
	q_5		
	q_6		$-2.54012 \cdot 10^{-1}$
$\beta^{(1)}$	q_1	$3.54664 \cdot 10^{-1}$	$-5.84290 \cdot 10^{1}$
	q_2		$1.04966 \cdot 10^{4}$
	q_3		$1.20107 \cdot 10^{1}$
	q_4	$-8.83332 \cdot 10^{-4}$	
	q_5		
	q_6		$1.15974 \cdot 10^{1}$
$\beta^{(2)}$	q_1	$9.97513 \cdot 10^{-2}$	$4.68200 \cdot 10^{-1}$
	q_2	$-1.33958 \cdot 10^{3}$	$7.73723 \cdot 10^{3}$
	q_3	$-4.79784 \cdot 10^{0}$	$5.99342 \cdot 10^{1}$
	q_4		$-1.14262 \cdot 10^{-1}$
	q_5	$4.23350 \cdot 10^{-6}$	
	q_6		
C^{ϕ}	q_1	$-1.71868 \cdot 10^{-3}$	$2.46063 \cdot 10^{-4}$
	q_2		$2.50262 \cdot 10^{1}$
	q_3	$-3.75585 \cdot 10^{-2}$	$1.95084 \cdot 10^{-1}$
	q_4	$1.26468 \cdot 10^{-4}$	$-3.71657 \cdot 10^{-4}$
	q_5		
	q_6		

Table 6. Parameters of eqs 20 to 22 for NaHCOO(aq)

	ΔH°_S, ${}^{\phi}C^\circ_P$		C°_P(s)[a]
p_1	$3.52859 \cdot 10^{5}$	p_5	$4.62450 \cdot 10^{1}$
p_2	$2.84944 \cdot 10^{2}$	p_6	$1.30472 \cdot 10^{-1}$
p_3	$-2.55974 \cdot 10^{-1}$	p_7	$-2.89788 \cdot 10^{-5}$
p_4	$-7.27402 \cdot 10^{4}$		

[a] Valid from (200 to 400) K.

$$\ln K_{MX} = 2\ln(m_{sat}/m^\circ) + 2\ln(\gamma_{MX,sat}) + \nu_0 \ln a_{w,sat} \quad (24)$$

Provided that reliable values of the molalities m_{sat} in saturated solutions are available, the present model can be used to calculate the thermodynamic solubility product. The solubilities in metal formate systems were recently reviewed by Balarew et al.[43] They reported a fairly consistent set of solubility measurements in the system (NaHCOO + H_2O) including stable solubility branches with respect to anhydrous NaHCOO and two hydrates, NaHCOO·$2H_2O$ and NaHCOO·$3H_2O$ (Figure 4). The solubility data were used together with the model parameters for NaHCOO(aq) listed in Table 5 to calculate values of the solubility products of the solids from eq 24. These values of ln *K* were then fitted to eq 19 to represent the temperature dependence of the solubility products. The fitting constants are listed in Table 7, and the calculated solubilities are depicted in Figure 4. The model represents the solubilities in the (NaHCOO + H_2O) system to within the experimental uncertainties.

The calculated invariant point NaHCOO·$3H_2O$ + ice + solution at 256.08 K and $m = 4.567$ mol·kg^{-1} is in reasonable agreement with both the solubilities reported by Groschuff[44] and the freezing temperatures of Sidgwick and Gentle.[33] Since the latter data were not included in the least-squares treatment, this is an indication that the model extrapolates well to low temperatures. The calculated invariant points NaHCOO·$3H_2O$ + NaHCOO·$2H_2O$ + solution ($T = 290.08$ K, $m = 11.25$ mol·kg^{-1}) and NaHCOO·$2H_2O$ + NaHCOO + solution ($T = 299.27$, $m = 14.76$ mol·kg^{-1}) are consistent with the experimental solubilities. Groschuff[44] reported transition temperatures of (290 and 298) K, respectively. Considering both the influence of the scatter in the experimental solubilities of NaHCOO·$2H_2O$ (Figure 4) and the experimental uncertainty of the early thermometric determinations by Groschuff, there is reasonable agreement between the experimental and the calculated transition temperatures.

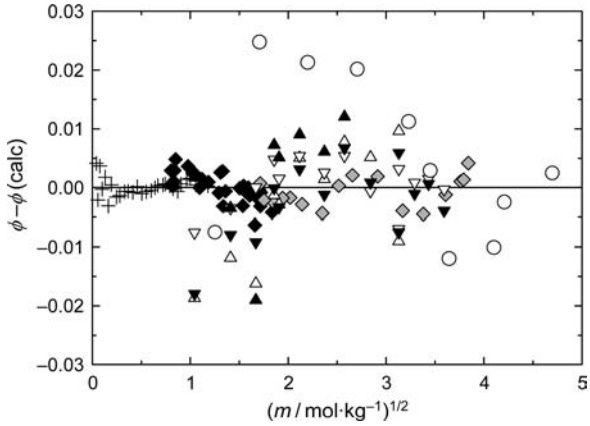

Figure 2. Deviations of the experimental osmotic coefficients of NaHCOO(aq) from the model as a function of the square root of molality using parameters of Table 5. Experimental data are: +, the freezing temperatures of Scatchard and Prentiss;[34] ♦, the isopiestic data at 298.15 K of Smith and Robinson;[28] gray ◊, the isopiestic data at 298.15 K of Bonner;[29] ○, the vapor pressure data at 373.15 K of Tammann.[32] The remaining symbols represent the vapor pressure data of this work at: △, 278.15 K; ▲, 288.15 K; ▼, 298.15 K; ▽, 308.15 K.

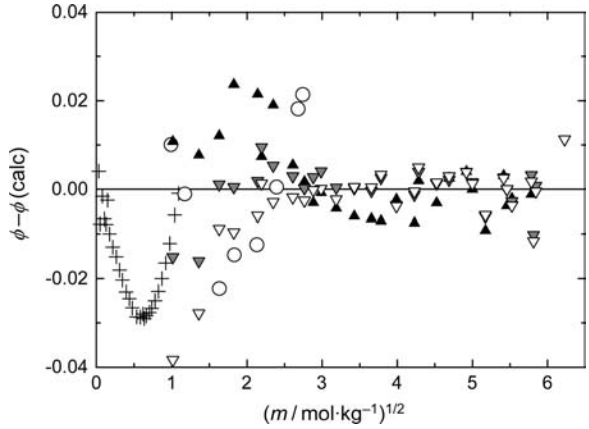

Figure 3. Deviations of the experimental osmotic coefficients of KHCOO(aq) from the model as a function of the square root of molality using parameters of Table 6. Experimental data are: +, the freezing temperatures of Scatchard and Prentiss;[34] ○, vapor pressure data at 373.15 K of Tammann.[32] The remaining symbols represent the vapor pressure data of this work at: △, 278.15 K; ▲, 288.15 K; gray ▽, 298.15 K; ▽, 308.15 K.

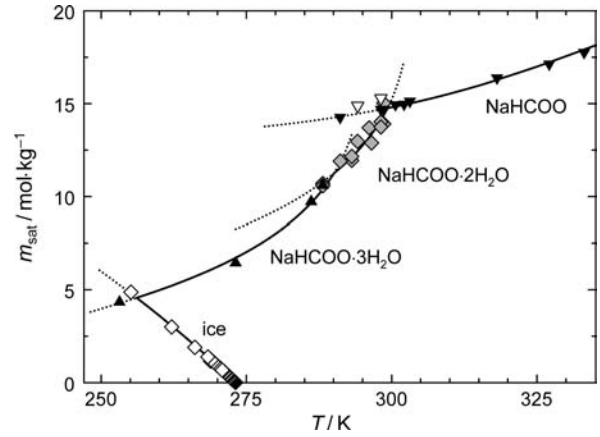

Figure 4. Experimental and calculated solubilities and freezing temperatures in the system NaHCOO + H_2O. Symbols refer to: ◊, experimental freezing temperatures of NaHCOO·$3H_2O$;[33,34] ▲, solubilities[43] of NaHCOO·$3H_2O$; gray ◊, solubilities of NaHCOO·$2H_2O$;▼, solubilities of NaHCOO (open inverted triangles not included in fit).

Table 7. Parameters of eqs 19 and 24 for ln K of NaHCOO, NaHCOO·$2H_2O$, NaHCOO·$3H_2O$, and KHCOO[a]

	NaHCOO	NaHCOO·$2H_2O$	NaHCOO·$3H_2O$	KHCOO
q_1	5.152922	3.931292	3.544442	8.184612
q_2	−4242.709	−2521.199	−3433.416	2150.962
q_3	−15.09769			6.058341

[a] $q_4 = q_5 = q_6 = 0$.

Much less solubility data are available for the (KHCOO + H_2O) system, and the data listed in the compilation of Balarew et al.[43] are substantially scattered. Apart from the anhydrous solid, no additional hydrated phases have been reported. Following Balarew et al.,[43] we accepted the solubilities of Groschuff[44] and calculated values of ln *K* for KHCOO that were then fitted to eq 19 in the temperature range (253 to 323) K. The fitting constants are listed in Table 7. Figure 5 depicts calculated solubilities and freezing temperatures in comparison to the experimental data. It should be noted that only the freezing temperatures of Scatchard and Prentiss[34] were used in the determination of the model parameters. These data were measured for rather dilute solutions ($m < 1.2$ mol·kg^{-1}) and extend to only 269 K. Nonetheless, there is reasonable agreement with the experimental freezing temperatures in more concentrated solutions of both Sidgwick and Gentle[33] and Aittomäki and Lahti.[7] Also the calculated solubility curve at temperatures below 253 K shows reasonable behavior; thus, some extrapolation to low temperatures appears possible, while the model cannot be used at temperatures above 323 K due to

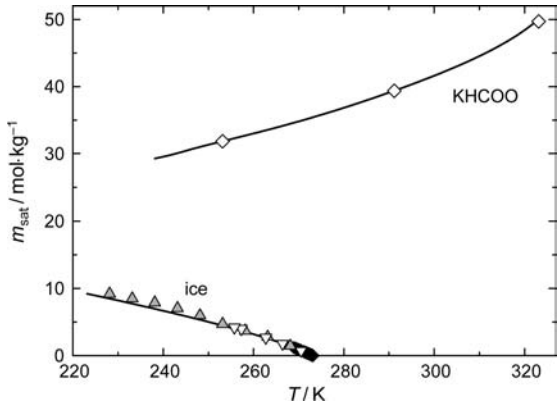

Figure 5. Experimental and calculated solubilities and freezing temperatures in the system KHCOO + H_2O. Symbols refer to solubilities[43] of KHCOO (open diamonds) and experimental freezing temperatures of Scatchard and Prentiss[34] (black diamonds), Sidgwick and Gentle[33] (open inverted triangle), and Aittomäki and Lahti[7] (grey triangles).

the extremely high solubility of KHCOO, requiring considerable extrapolation of the ion interaction equations.

Conclusions

The vapor pressure measurements in this work are consistent with available thermodynamic data of NaHCOO(aq) and KHCOO(aq). The extended Pitzer type ion interaction equations presented here provide an accurate calculation of activity coefficients and water activities at near ambient temperatures to very high concentration. The thermodynamic database is reasonable and fairly accurate for sodium formate, allowing for the calculation of solubilities and freezing temperatures from the eutonic temperature at 256 K to about 330 K. In contrast, the database for potassium formate is quite inadequate. There is a lack of thermochemical data over the entire temperature range, and activity data are not available at subzero and at enhanced temperatures. Also, the available solubility database is incomplete and badly scattered. The model equations for KHCOO(aq) provided here are useful to represent the thermodynamic properties and phase equilibria at near ambient temperatures. Given the large number of applications of this salt at low temperatures, additional measurements are required.

Literature Cited

(1) Wiener, H.; Sasson, Y.; Blum, J. Palladium catalyzed decomposition of aqueous alkali metal formate solutions. *J. Mol. Catal.* **1986**, *35*, 277–284.

(2) Klingler, R. J.; Rathke, J. W. Catalytic conversion of CO and H_2O to alcohols. *Am. Chem. Soc., Div. Pet. Chem., Prepr.* **1986**, *29*, 596–601.

(3) Engel, D. C.; Versteeg, G. F.; van Swaaij, W. P. M. Chemical equilibrium of hydrogen and aqueous solutions of 1:1 bicarbonate and formate salts with a common cation. *Fluid Phase Equilib.* **1997**, *135*, 109–136.

(4) Zaidman, B.; Wiener, H.; Sasson, Y. Formate salts as chemical carriers in hydrogen storage and transportation. *Int. J. Hydrogen Energy* **1986**, *11*, 341–347.

(5) Wiener, H.; Zaidman, B.; Sasson, Y. Storage of energy by solutions of alkali formate salts. *Sol. Energy* **1989**, *43*, 291–296.

(6) Königsberger, E.; Eriksson, G.; May, P. M.; Hefter, G. Comprehensive model of synthetic Bayer liquors. Part 1. Overview. *Ind. Eng. Chem. Res.* **2005**, *44*, 5804–5814.

(7) Aittomäki, A.; Lahti, A. Potassium formate as a secondary refrigerant. *Int. J. Refrig.* **1997**, *20*, 276–282.

(8) Riffat, S. B.; James, S. E.; Wong, C. W. Experimental analysis of the absorption and desorption rates of HCOOK/H_2O and LiBr/H_2O. *Int. J. Energy Res.* **1998**, *22*, 1099–1103.

(9) Robidoux, P. Y.; Delisle, C. E. Ecotoxicological evaluation of three deicers (NaCl, NaFo, CMA)—Effect on terrestrial organisms. *Ecotoxicol. Environ. Saf.* **2001**, *48*, 128–139.

(10) Hellstén, P. P.; Salminen, J. M.; Jørgensen, K. S.; Nystén, T. H. Use of potassium formate in road winter deicing can reduce groundwater deterioration. *Environ. Sci. Technol.* **2005**, *39*, 5095–5100.

(11) Peng, C.; Chan, C. K. The water cycles of water-soluble organic salts of atmospheric importance. *Atmos. Environ.* **2001**, *35*, 1183–1192.

(12) Sabbioni, C.; Ghendini, N.; Bonazza, A. Organic anions in damage layers on monuments and buildings. *Atmos. Environ.* **2003**, *37*, 1261–1269.

(13) Zehnder, K.; Arnold, A. Stone damage due to formate salts. *Stud. Conserv.* **1984**, *29*, 32–34.

(14) Ryhl-Svendsen, M.; Glastrup, J. Acetic acid and formic acid concentrations in the museum environment measured by SPME-GC/MS. *Atmos. Environ.* **2002**, *36*, 3909–3916.

(15) Tennent, N. H.; Baird, T. The deterioration of mollusca collections: Identification of shell efflorescences. *Stud. Conserv.* **1985**, *30*, 73–85.

(16) Beyer, R.; Steiger, M. Vapour pressure measurements and thermodynamic properties of aqueous solutions of sodium acetate. *J. Chem. Thermodyn.* **2002**, *34*, 1057–1071.

(17) Dorn, J.; Steiger, M. Measurement and calculation of solubilities in the ternary system $NaCH_3COO$ + NaCl + H_2O from 278 to 323 K. *J. Chem. Eng. Data* **2007**, *52*, 1784–1790.

(18) Gibson, L. T.; Cooksey, B. G.; Littlejohn, D.; Linnow, K.; Steiger, M.; Tennent, N. H. The mode of formation of thecotrichite, a widespread calcium acetate nitrate chloride efflorescence. *Stud. Conserv.* **2005**, *50*, 284–294.

(19) Linnow, K.; Halsberghe, L.; Steiger, M. Analysis of calcium acetate efflorescences formed on ceramic tiles in a museum environment. *J. Cult. Heritage* **2007**, *8*, 44–52.

(20) Pitzer, K. S. In *Activity Coefficients in Electrolyte Solutions*; Pitzer, K. S., Ed.; CRC Press: Boca Raton, FL, 1991; pp 75−153.

(21) Pitzer, K. S.; Mayorga, G. Thermodynamics of electrolytes. III. Activity and osmotic coefficients for 2−2 electrolytes. *J. Solution Chem.* **1974**, *3*, 539–546.

(22) Steiger, M. Crystal growth in porous materials: I. The crystallization pressure of large crystals. *J. Cryst. Growth* **2005**, *282*, 455–469.

(23) Steiger, M.; Kiekbusch, J.; Nicolai, A. An improved model incorporating Pitzer's equations for calculation of thermodynamic properties of pore solutions implemented into an efficient program code. *Constr. Build. Mater.* **2008**, *22*, 1841–1850.

(24) Steiger, M.; Asmussen, S. Crystallization of sodium sulfate phases in porous materials: the phase diagram Na_2SO_4-H_2O and the generation of stress. *Geochim. Cosmochim. Acta* **2008**, *72*, 4291–4306.

(25) Rard, J. A.; Platford, R. F. In *Activity Coefficients in Electrolyte Solutions*; Pitzer, K. S., Ed.; CRC Press: Boca Raton, FL, 1991; pp 209−277.

(26) Kell, G. S. Effects of isotopic composition, temperature, pressure, and dissolved gases on the density of liquid water. *J. Phys. Chem. Ref. Data* **1977**, *6*, 1109–1131.

(27) Saul, A.; Wagner, W. International equations for the saturation properties of ordinary water substance. *J. Phys. Chem. Ref. Data* **1987**, *16*, 893–901.

(28) Smith, E. R. B.; Robinson, R. A. The vapour pressures and osmotic coefficients of solutions of the sodium salts of a series of fatty acids at 25 °C. *Trans. Faraday Soc.* **1942**, *38*, 70–78.

(29) Bonner, O. D. Osmotic and activity coefficients of the sodium salts of formic, acetic and propionic acids. *J. Solution Chem.* **1988**, *17*, 999–1002.

(30) Archer, D. G. Thermodynamic properties of the KCl + H_2O system. *J. Phys. Chem. Ref. Data* **1999**, *28*, 1–16.

(31) Hamer, W. J.; Wu, Y.-C. Osmotic coefficients and mean activity coefficients of uni-univalent electrolytes in water at 25 °C. *J. Phys. Chem. Ref. Data* **1972**, *1*, 1047–1099.

(32) Tammann, G. Die Dampftensionen der Lösungen. *Z. Phys. Chem.* **1888**, *2*, 42–47.

(33) Sidgwick, N. V.; Gentle, J. A. H. R. The solubilities of the alkali formates and acetates in water. *J. Chem. Soc.* **1922**, *121*, 1837–1843.

(34) Scatchard, G.; Prentiss, S. S. The freezing points of aqueous solutions. VI. Potassium, sodium and lithium formates and acetates. *J. Am. Chem. Soc.* **1934**, *56*, 807–811.

(35) Klotz, I. M.; Rosenberg, R. M. *Chemical thermodynamics, basic theory and methods*, 3rd ed.; Benjamin/Cummings: Menlo Park, CA, 1972; pp 37 −378.

(36) Snell, H.; Greyson, J. Water structure in solutions of the sodium salts of some aliphatic acids. *J. Phys. Chem.* **1970**, *74*, 2148–2152.

(37) Chawla, B.; Ahluwalia, J. C. Enthalpies and heat capacities of dissolution of some sodium carboxylates in water and hydrophobic hydration. *J. Solution Chem.* **1975**, *4*, 383–389.

(38) Ackermann, T.; Schreiner, F. Molwärmen und Entropien einiger Fettsäuren und ihrer Anionen in wässriger Lösung. *Z. Elektrochem.* **1958**, *62*, 1143–1151.

(39) Kell, G. S. Density, thermal expansitivity, and compressibility of liquid water from 0° to 150 °C: Correlations and tables for atmospheric

pressure and saturation reviewed and expressed on 1968 temperature scale. *J. Chem. Eng. Data* **1975**, *20*, 97–105.
(40) Westrum, E. F.; Chang, S.-S.; Levitin, N. E. The heat capacity and thermodynamic properties of sodium formate from 5 to 350 K. *J. Phys. Chem.* **1960**, *64*, 1553–1554.
(41) Franzosini, P.; Plautz, W. A.; Westrum, E. F. Thermophysics of metal alkanoates 1. Heat capacities and thermodynamic properties of sodium methanoate and ethanoate. *J. Chem. Thermodyn*. **1983**, *15*, 445–456.
(42) Archer, D. G.; Wang, P. The dielectric constant of water and Debye-Hückel limiting law slopes. *J. Phys. Chem. Ref. Data* **1990**, *19*, 371–411.
(43) Balarew, C.; Dirkse, T.; Golubchikov, O. A.; Salomon, M. IUPAC-NIST solubility data series. 73. Metal and ammonium formate systems. *J. Phys. Chem. Ref. Data* **2001**, *30*, 1–163.
(44) Groschuff, E. Neutrale und saure Alkaliformiate. Studien über die Löslichkeit der Salze. *Ber. Dtsch. Chem. Ges.* **1903**, *36*, 1783–1795.

Received for review June 9, 2009. Accepted August 1, 2009. Financial support of this research by the European Commission (Grant No. ENV4-CT95−0135) is gratefully acknowledged.

JE900487A